

Supporting Information for:

The Nature of the Interlayer Interaction in Bulk and Few-Layer Phosphorus

L. Shulenburger,[†] A.D. Baczewski,[†] Z. Zhu,[‡] J. Guan,[‡] and D. Tománek^{*,‡}

[†]*Sandia National Laboratories, Albuquerque, New Mexico 87185, United States*

[‡]*Physics and Astronomy Department, Michigan State University, East Lansing, Michigan
48824, United States*

E-mail: tomanek@pa.msu.edu

VASP calculations

With the exception of the DFT calculations used to generate the trial wavefunctions for the Diffusion Monte Carlo (DMC) technique, all Density Functional Theory (DFT) results reported in the manuscript have been generated using the Vienna Ab Initio Software Package (VASP).^{S1-S3} The calculations were performed using the P-GW Projector Augmented Wave (PAW) potentials for phosphorus taken from the 2012 PBE PAW set. VASP is able to re-evaluate the PAW for use with other functionals, so the same PAW is used for all calculations. A plane wave cutoff of 500 eV was used for all calculations. Calculations on bulk phosphorus utilized a $12 \times 12 \times 6$ Γ -centered k-point set, whereas calculations for the isolated slab and bilayers utilized a $12 \times 12 \times 1$ k-point set. For isolated and bilayer geometries, the cell was 20 Å in the direction perpendicular to the layers (the c axis). Results were checked with a 40 Å cell and relative energies were found to be converged to less than 0.1 meV/atom.

Convergence of Finite-Size Effects in Quantum Monte Carlo

One- and two-body finite size effects must be considered in both the bulk and planar periodic structures. One-body effects are corrected using canonical twist averaging,^{S4} while two-body effects are extrapolated. Controlling the two-body effects presents a challenge for extrapolation consistent with reports of calculations done on graphite.^{S5}

For bulk systems, we consider two types of tilings for generating these supercells. We expect finite-size effects to converge more quickly when increasing the effective system size along the layering axis rather than in-plane. Consequently, we study two-body effects for $2\times 2\times 1$, $3\times 3\times 1$, $4\times 4\times 1$, and $5\times 5\times 1$ tilings (i.e., a single AB bilayer per supercell) and $2\times 2\times 2$, $3\times 3\times 2$, and $4\times 4\times 2$ tilings (i.e., two AB bilayers per supercell).

The peculiar nature of the electron correlation in two-dimensional systems such as black phosphorus, coupled with the meV accuracy required for this study, requires a slightly different procedure for assessing and reducing the two-body finite-size effects introduced by simulating a supercell with periodic boundary conditions. The procedures commonly used to achieve this either utilize a model interaction that removes spurious electron correlation,^{S6} analyze the behavior of the structure factor and two body Jastrow factor for small values or momentum transfer,^{S7} or utilize calculations with density functionals designed to mimic the energetics of the electron correlation in finite supercells.^{S8} As generally practiced, all of these procedures rely on the assumption that the electron correlation is isotropic, a condition that is grossly violated in a layered material like black phosphorus.

This difficulty has been noted in previous quantum Monte Carlo (QMC) studies of layered materials,^{S5} where a combination of the KZK functional^{S8} was used for correlations in the plane, and an extrapolation scheme was used for correlations in the direction perpendicular to the planes. Our approach is to extend this methodology in two regards. Firstly, we utilize extrapolation in the size of the supercell to determine correlations both in plane and out of

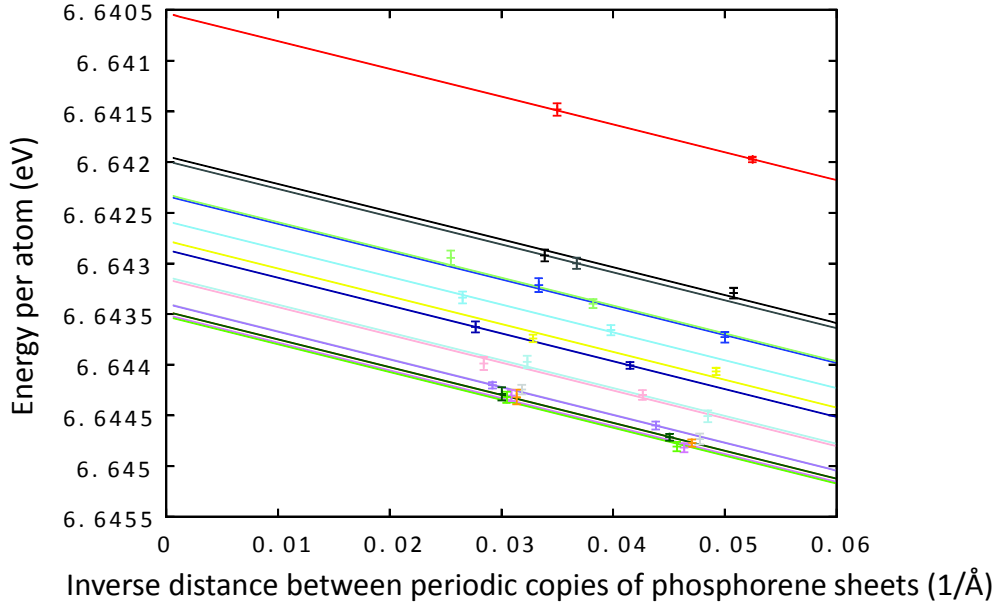


Figure S1: Energy per atom of black phosphorus as a function of the inverse of the shortest distance between periodic images of phosphorene sheets. The identical slope of the lines enforces consistency in the extrapolation for calculations, where the distance between adjacent sheets is varied.

plane and secondly, because such extrapolations can introduce a significant amount of noise in the extrapolated quantities, we correlate the parameters of the extrapolations between systems with similar geometries. This is best illustrated looking at the extrapolation of the energy in the direction perpendicular to the phosphorene planes.

This correlation may be expected to decrease with distance between the planes and also be a function of the number of layers simulated. To capture this, we extrapolate based on the total distance between images in the perpendicular direction and also require that the slope of the extrapolation be a simple function of the distance between the planes. The results of this procedure are shown in Figure S1, where the energy per atom for different supercells with different spacings between the phosphorene planes and different numbers of layers in the supercell are shown as a function of the inverse of the distance between the top and bottom of the supercell. All of these calculations had a 3×3 tiling of the primitive cell of phosphorus in the direction parallel to the planes and both the spacing between the layers and the number of copies of the supercell were varied. A similar procedure was used

to extrapolate to infinitely large supercells in the other direction.

Numerical Considerations in QMC

To control the computational cost, we verify that our choice of DMC time step satisfies a balance between efficient sampling and having a large time-step bias. In doing so, for each system we choose fixed, moderately sized supercells and perform short DMC runs using different time steps. A best-fit line is constructed for the energy as a function of the time step. We then use the largest time step that is within 1 mHa/atom of the zero time-step extrapolated energy. We have found that a time step of 0.0075 a.u. is adequate to achieve this level of accuracy in all cases.

Further, to control the memory required by the wave function, we assess the effect of enlarging the grid spacing associated with the B-spline representation of the Kohn-Sham orbitals relative to the equivalent real space grid used in the plane wave pseudopotential calculation, in which they have been generated. The convergence of the total energy, kinetic energy, and variance in the local energy are assessed in determining the appropriate grid spacing. Noting that the variance converges most slowly in the grid spacing, an enlargement factor of 4/3 preserves accuracy while reducing the memory used up in representing the wave function.

Pseudopotential Generation and Testing

Two different pseudopotentials were generated for this study, one treating 5 valence electrons and the other treating 13. Both pseudopotentials were generated using the OPIUM pseudopotential generation code.^{S9} The benchmark quantities under consideration are the equilibrium properties of a phosphorus dimer and the ionization potential and electron affinity of an isolated phosphorus atom.

In Table S1 we provide some atomic benchmarks. While the accuracy of the two pseu-

dopotentials relative to experiment is comparable for the ionization potential, the 5-electron pseudopotential performs worse for the electron affinity. Given the relatively primitive trial wavefunction used, these results should not be taken as conclusive. Still, we expect errors due to the nodal surface to cause inaccuracies of less than a few tenths of an eV.

Table S1: Ionization potential and electron affinity of an isolated phosphorus atom computed using two different pseudopotentials. Experimental values for the ionization potential and electron affinity are taken from References S10 and S11, respectively.

	5 electron	13 electron	Experiment
Ionization Potential	10.7112 ± 0.00084	10.6832 ± 0.0598	10.48669
Electron Affinity	0.6405 ± 0.0084	0.7483 ± 0.0626	0.746609

We also calculate the binding energy, atomization energy and vibrational frequency of the phosphorus dimer by determining the energy as a function of bond length. The results of these calculations for each pseudopotential and a fit to a Morse potential are shown in Figure S2. The corresponding resulting observables are summarized in Table S2.

Table S2: Properties of phosphorus dimer computed using two different pseudopotentials. The experimental bond length, vibrational frequency and atomization energy are taken from references S12, S13 and S12, respectively.

	5 electron	13 electron	Experiment
bond length (\AA)	1.8618 ± 0.009	1.8824 ± 0.0018	1.89340 ± 0.00044
vibrational frequency (cm^{-1})	827.3 ± 9.4	851.7 ± 31.8	780.77
atomization energy (eV)	4.900 ± 0.001	4.894 ± 0.040	5.03 ± 0.02

While both the 5-electron and 13-electron pseudopotentials have similar accuracy relative to experiment, calculations using the potential with 13 electrons in the valence are nearly 100 times more expensive than those using the 5-electron potential. Therefore, its success in these metrics leads us to use the 5-electron pseudopotential for all remaining calculations on bulk phosphorus and phosphorene.

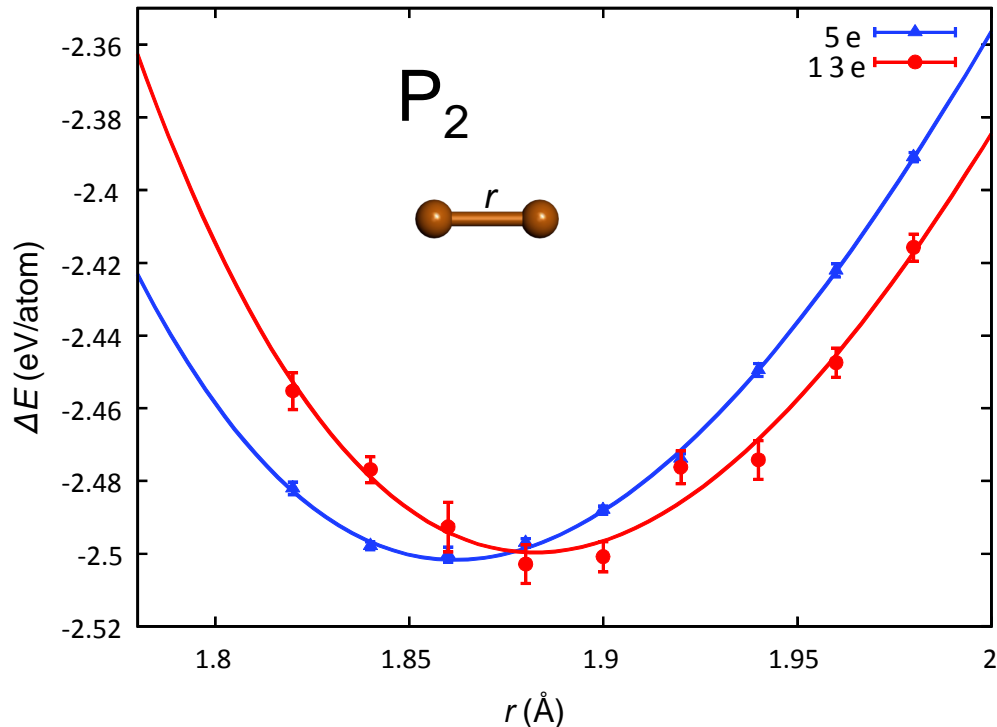


Figure S2: Energy of a phosphorus dimer as a function of the bond length obtained using 5- and 13-electron pseudopotentials.

AA and AB Bilayer Energetics

Here we provide binding curves for the same functionals presented in Figure 1 of the main manuscript for the AA-stacked bilayer.

We are not surprised to find that all the functionals predict that the AB stacking is more stable than the AA stacking, and that all functionals predict that the AA stacking is metastable. The energy difference between the two stackings is generally underestimated relative to DMC. DMC also predicts that the change in the equilibrium interlayer spacing is larger than predicted by all DFT functionals. As in the main text of the paper, the sequence of LDA, PBE, TPSS, and PBE0 are presented to illustrate the effect of different treatments of exchange on increasing levels of the “Jacob’s ladder”,^{S14} and that these functionals are not expected to get the correct interlayer binding without being augmented with vdW corrections.

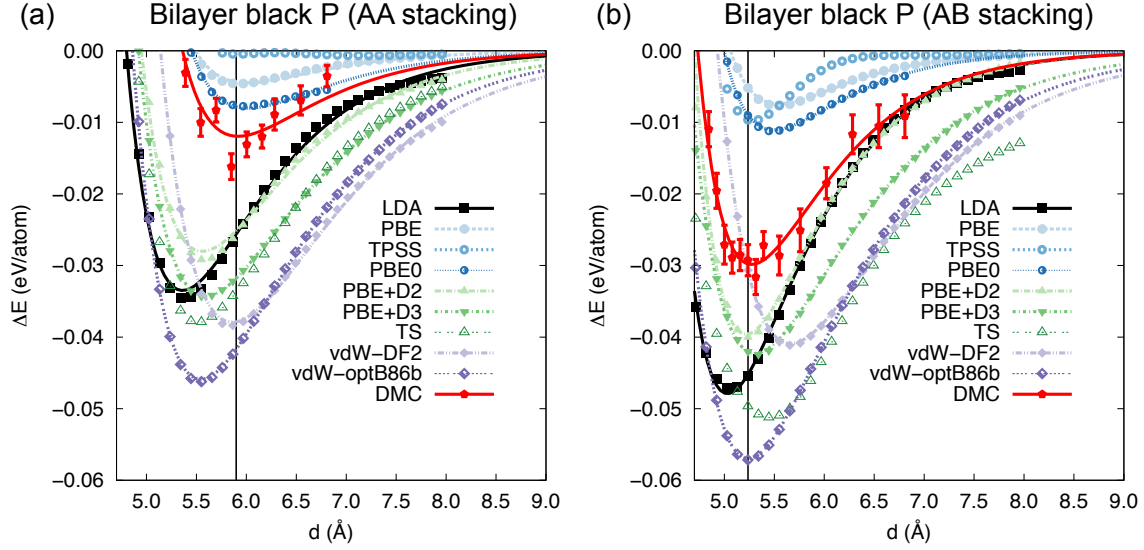


Figure S3: Binding energies of the AA (left) and AB (right) stackings of bilayer phosphorene for the same group of functionals assessed in the paper.

References

- [S1] Kresse, G.; Furthmüller, J. *Phys. Rev. B* **1996**, *54*, 11169–11186.
- [S2] Kresse, G.; Furthmüller, J. *Comp. Mat. Sci.* **1996**, *6*, 15–50.
- [S3] Kresse, G.; Joubert, D. *Phys. Rev. B* **1999**, *59*, 1758–1775.
- [S4] Lin, C.; Zong, F.; Ceperley, D. *Phys. Rev. E* **2001**, *64*, 016702.
- [S5] Spanu, L.; Sorella, S.; Galli, G. *Phys. Rev. Lett.* **2009**, *103*, 196401.
- [S6] Fraser, L. M.; Foulkes, W. M. C.; Rajagopal, G.; Needs, R. J.; Kenny, S. D.; Williamson, A. J. *Phys. Rev. B* **1996**, *53*, 1814–1832.
- [S7] Chiesa, S.; Ceperley, D.; Martin, R.; Holzmann, M. *Phys. Rev. Lett.* **2006**, *97*, 076404.
- [S8] Kwee, H.; Zhang, S.; Krakauer, H. *Phys. Rev. Lett.* **2008**, *100*, 126404.
- [S9] OPIUM pseudopotential package,
<http://opium.sourceforge.net> (accessed 19 October 2015).

- [S10] Peláez, R. J.; Blondel, C.; Vandevraye, M.; Drag, C.; Delsart, C. *J. Phys. B: At., Mol. Opt. Phys.* **2011**, *44*, 195009.
- [S11] Svendenius, N. *Phys. Scr.* **1980**, *22*, 240–287.
- [S12] Huber, K.-P.; Herzberg, G. *Constants of diatomic molecules*; Van Nostrand Reinhold Company: New York, N.Y., USA, 1979.
- [S13] Irikura, K. K. *J. Phys. Chem. Ref. Data* **2007**, *36*, 389–397.
- [S14] Perdew, J. P.; Schmidt, K. Jacob’s ladder of density functional approximations for the exchange-correlation energy. AIP Conference Proceedings. 2001; pp 1–20.